



ORIGINAL ARTICLE

Structural Implications of Transverse Openings in Reinforced Concrete Beams: Experimental and Analytical Studies

*¹Jen Hua Ling, ¹Howe Sheng Tang, ¹Yong Tat Lim and ¹Wen Kam Leong

¹Centre for Research of Innovation & Sustainable Development, School of Engineering and Technology, University of Technology Sarawak, 96000 Sibul, Sarawak, Malaysia

ABSTRACT - Transverse openings in reinforced concrete beams are often required for the passage of utility pipes and service ducts; however, they significantly affect structural performance. This study examined the impact of opening size and position on beam performance under shear and flexural loads using experimental and analytical methods. Eleven specimens with circular openings of 50 mm, 75 mm, and 100 mm in diameter were tested. The openings were positioned at 300 mm (one beam height from the support) and 750 mm (at the beam's midspan). The study assessed load-displacement responses, mechanical properties, deflections, and failure modes in comparison to solid beams. Three specimens, each using a different opening reinforcement method, were evaluated for reinforcement effectiveness. Results showed that openings reduced beam stiffness, yield strength, and ultimate strength, with larger, near-support, and inadequately reinforced openings causing more severe reductions. The diagonal bar reinforcement method effectively mitigated these effects for openings up to 1/3 of the beam height. Derived equations conservatively predicted load capacity with a mean strength ratio of 0.68, while accurately predicting failure modes with 90.9% reliability. Future research may explore the model's applicability to beams with multiple and large openings of various shapes.

ARTICLE HISTORY

Received: 02 Aug 2024

Revised: 10 Sept 2024

Accepted: 27 Dec 2024

KEYWORDS

*Reinforced concrete beam,
Circular transverse opening,
Flexural and shear loads,
Experimental and analytical studies.*

INTRODUCTION

Transverse openings are typically provided in reinforced concrete (RC) beams to allow the passage of mechanical and electrical services. This design alleviates constraints related to headroom or ceiling space and reduces the required lengths of pipes and ducts.

However, the provision of openings can adversely affect the beam's structural performance, leading to reduced strength, stiffness, and increased deflection [1-7]. These effects become more pronounced as the opening size increases [8-10]. The presence of openings removes concrete from the beam and disrupts its cross-sectional configuration, resulting in stress concentration around the opening and potentially premature failure under load [2, 11].

These structural deficiencies weaken individual beams, compromising the building's overall integrity, especially in continuous or composite systems. To minimize the impact on structural performance, the size of the opening should be small enough to maintain the beam-type behaviour, where beam theory remains applicable [1, 12]. Previous studies have recommended that circular openings should not exceed 0.25 and 0.2 times the beam's depth [13-14]. For rectangular openings, it is suggested that the maximum height and width should be 0.2 and 0.05 times the beam's depth and length, respectively [15]. Despite these guidelines, the understanding of RC beams with openings remains fragmented, and a comprehensive design guide is still lacking.

Circular openings generally perform better than square and rectangular ones, as stress is more uniformly distributed along the edges, avoiding concentration at sharp corners [16-19]. Openings are best placed at beam's mid-span rather than near the supports [20-21]. The critical impact is under shear load rather than

*Corresponding Author: Jen Hua Ling. University of Technology Sarawak (UTS), email: lingjenhua@uts.edu.my

flexural load [18], and openings should be avoided in regions with maximum deflection and shear load [5, 22]. Proper reinforcement methods, including internal and external strengthening, can help distribute stress, control crack propagation, and restore strength to levels comparable to solid beams [11, 23-25].

This study investigates the behaviour of RC beams with circular openings. The effects of opening size and position on beam performance are observed, and the effectiveness of different reinforcing methods is evaluated. Equations are derived to predict the ultimate load capacity and failure mode of the beams, and these equations are validated against experimental results.

MATERIALS AND METHODOLOGY

Specimen Details

Eleven RC beams were tested using a four-point load test (Figure 1 and Table 1), comprising:

- 2 control beams without openings
- 6 beams with unreinforced openings
- 3 beams with reinforced openings

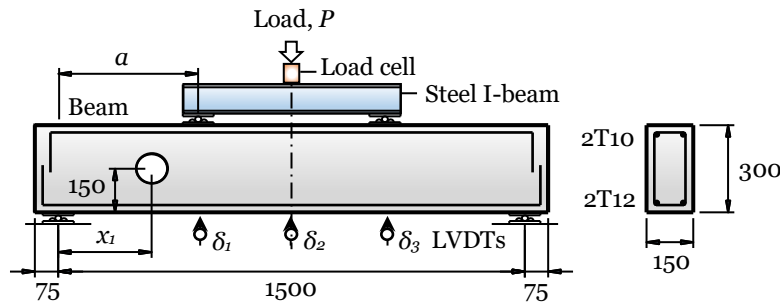


Figure 1. Test setup

Table 1. Details of specimen

Specimen*	Transverse opening		Point load	Shear reinforcement	Remarks
	Diameter, d_o (mm)	Distance from support, x_1 (mm)	Distance from support, a (mm)		
C1/S	-	-	500	R8-250	Control, shear
C2/F	-	-	600	R8-150	Control, flexural
S1/100	100	300	500	R8-250	Shear
S2/75	75	300	500	R8-250	Shear
S3/50	50	300	500	R8-250	Shear
F1/100	100	750	600	R8-150	Flexural
F2/75	75	750	600	R8-150	Flexural
F3/50	50	750	600	R8-150	Flexural
R1/DR	100	300	500	R8-250	Shear, reinforced
R2/GI	100	300	500	R8-250	Shear, reinforced
R3/DS	100	300	500	R8-250	Shear, reinforced

C – control, S – shear, F – flexural, R – reinforcement to opening

The specifications of the specimens were:

- Beam size : 150 mm (Width) x 300 mm (Height) x 1650 mm (Length)
- Clear span : 1500 mm
- Reinforcements : 2T12 bottom bars and 2T10 top bar
: Nominal yield strength, $f_{y,b} = 460 \text{ N/mm}^2$
- Shear links : R8-150 and R8-250 for flexural and shear tests, respectively
: Nominal yield strength, $f_{y,sl} = 250 \text{ N/mm}^2$
- Concrete cover : 25 mm

The beam specimens were horizontally cast in plywood moulds using ready-mixed concrete with the following properties:

- Grade : 25 N/mm²
- Designed slump : 60 mm – 180 mm
- Curing conditions : at least 7 days at the atmospheric temperature of $30 \pm 5^\circ\text{C}$
- Testing age : at least 28 days

Polyvinyl Chloride (PVC) pipes were used to create the transverse openings. These were placed at the beam's mid-height (150 mm from the soffit) at distances of 300 mm (representing one times the beam height) and 750 mm (representing the beam's mid-span) from the support (Figure 1). The opening sizes were 50 mm, 75 mm, and 100 mm.

The beams were tested for shear and flexural failures. To promote shear failure, the point loads were placed closer to the support ($a = 500$ mm), and fewer shear links (R8-250) were provided. A smaller distance a increased the shear load, while fewer shear links reduced the shear resistance, ensuring shear failure at the support. For flexural failure, the distance a and the shear links were set to 600 mm and R8-150, respectively. The increased distance a promoted flexural failure at mid-span, where bending stresses are higher, while the denser shear links provided adequate shear resistance to prevent shear failure at the supports. This approach ensured that both shear and flexural failure modes were achieved in the study.

Three opening reinforcement methods were tested under shear load: diagonal bar reinforcement, Galvanized Iron (GI) pipe, and diagonal square reinforcement (Figure 2). The reinforcement bars were placed at a 25 mm offset distance from the transverse opening, and the GI pipe replaced the PVC pipe. Each reinforcement method represented a specific scenario: the diagonal bar reinforcement was employed to control the development of potential cracks at the opening, the GI pipe strengthened the opening itself, and the diagonal square reinforcement simulated transverse reinforcement to confine the area around the opening. The effectiveness of these reinforcement methods was evaluated.

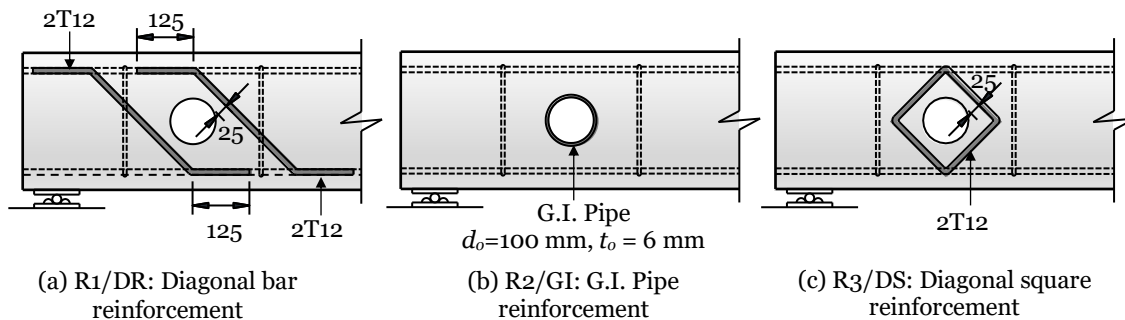


Figure 2. Proposed reinforcement for transverse opening

Test setup

A hydraulic cylinder applied a static load, distributed into two point loads acting on the beam by a steel I-beam (Figure 3). A load cell was placed between the hydraulic cylinder and the steel I-beam to measure the load. Three linear variable differential transducers (LVDTs) measured the vertical displacement of the beam at the mid-span and below the two-point loads. All measuring devices were connected to a data logger for data acquisition (Table 2).

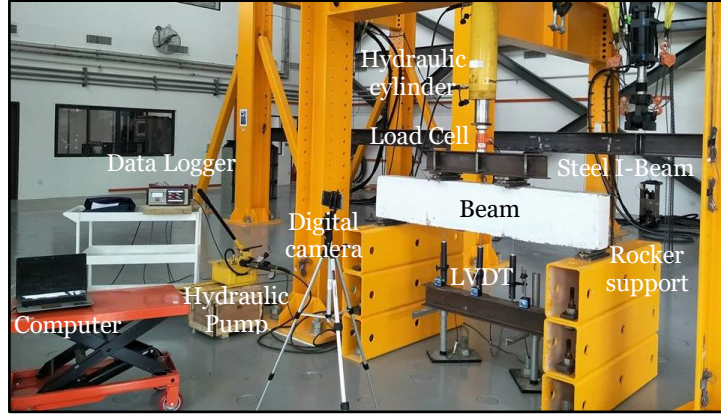


Figure 3. Experimental setup in the laboratory

Table 2. Instrument specifications

Instruments	Brand, Model	Description	Data Accuracy
Hydraulic Cylinder	Enerpac, RR-10018	Push +933kN, Pull -435kN	-
Hydraulic Pump	Enerpac P464	Manual hand pump	-
Displacement transducer	TML, CDP-100	100 mm	0.01 mm
Load Cell	TML, CLJ-300KNB	Capacity 300kN	0.01 kN
Data Logger	TML, TDS-530	30 Channels	-

Test procedure

Before testing, all readings were set to zero. The beam was preloaded to not more than 10% of the estimated beam capacity for about 5 minutes to consolidate the test setup. The load was then released for another 5 minutes to ensure the readings returned to zero, verifying the validity of the measuring devices. This process was repeated twice.

The test commenced after reinitializing the readings to zero. The load was manually increased using a hand pump at a slow and steady rate, with increments monitored at intervals of 7 kN or 0.5 mm, whichever was reached first. Although the exact incremental rate of loading was not measured, care was taken to ensure consistent progression. The load was held for at least 1 minute before readings were taken. The load-displacement response of the beam and the propagation of cracks were monitored throughout the test. The beam was considered failed after three consecutive drops in the load reading, marking the end of the test.

TEST RESULTS

The test results are presented in terms of (a) the properties of the materials used, (b) the specimens' test results obtained during the experiments, (c) the beam properties extracted from the load-displacement response, and (d) the beams' performance ratios computed from the test results and beam properties.

Material properties

A 150 mm concrete cube was tested under compressive load on the same day the beam specimens were tested to represent the compressive strength of the concrete in the beams. The compressive strengths were consistent and met the design strength of 25 N/mm² (Table 3).

Three samples of high-yield steel and mild steel bars were tested under tensile load to represent the main reinforcement and the shear links used in the beam specimens. The steel strengths were consistently higher than their nominal strengths of 460 N/mm² and 250 N/mm², respectively (Table 4).

Given these results, the quality of the materials was considered acceptable, and the influence of inconsistent material quality on the test results of the specimens was deemed minimal.

Table 3. Test results of concrete cubes representing different test specimens

Testing day	Specimen	Compressive strength, $f_{c,u}$ (N/mm ²)	Density ρ_c (kg/m ³)
28	C1/S	25.1	2320
29	C2/F	25.9	2329
30	S1/100	24.7	2320
31	S2/75	24.9	2367
35	S3/50	25.4	2344
36	F1/100	25.7	2329
37	F2/75	25.0	2347
38	F3/50	26.9	2335
42	R1/DR	26.7	2367
43	R2/GI	26.2	2320
44	R3/DS	25.8	2373

Table 4. Experimental result of tensile strength

Bar type	Tensile strength (N/mm ²)			Average strength (N/mm ²)
	Sample 1	Sample 2	Sample 3	
High-yield steel bar	532	551	547	543
Mild steel bar	295	281	278	285

Experimental results

Table 5 presents the test results of the specimens. The cracking loads ($P_{ic,s}$, $P_{ic,f}$, and $P_{ic,o}$) were identified upon detection of the respective cracks during the tests (Figure 4). The failure mode (flexural or shear failure) was determined based on the severity of the cracks.

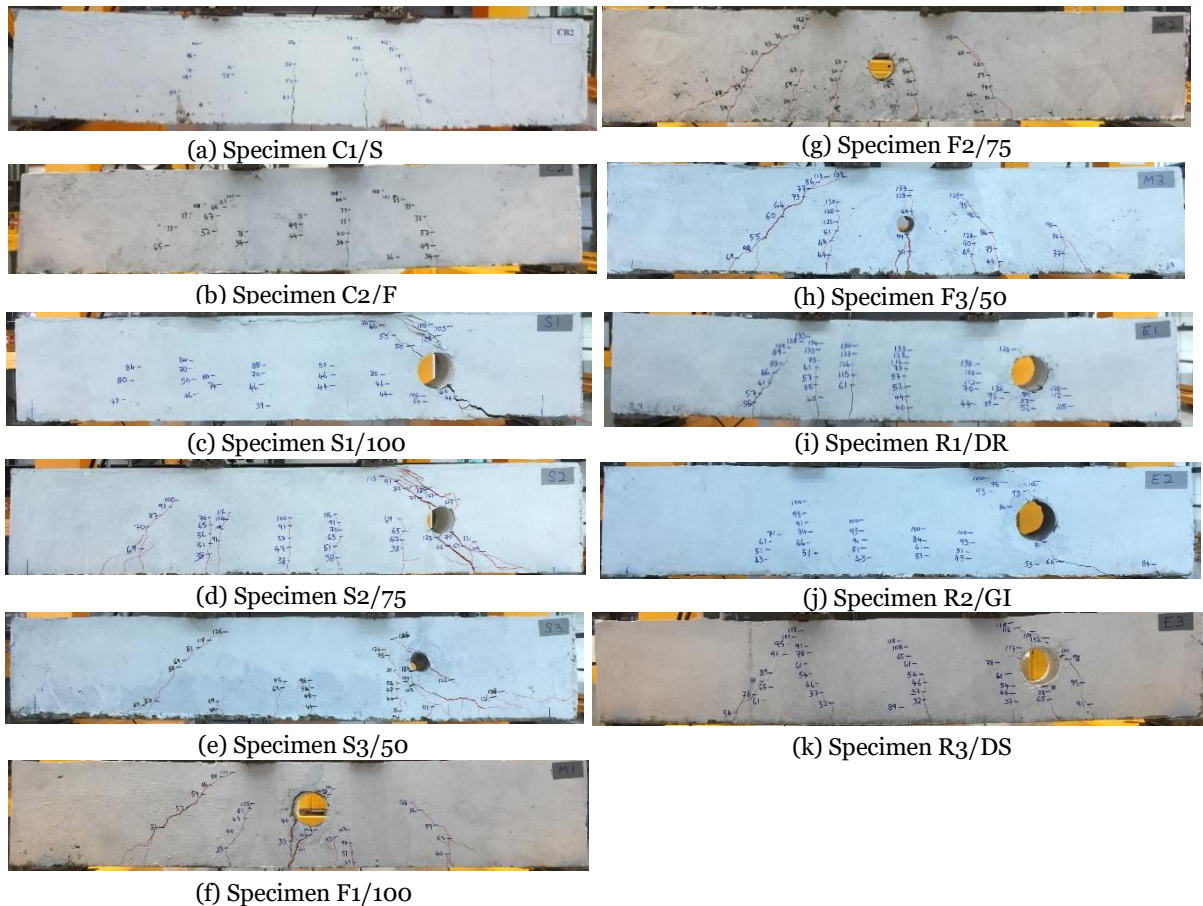


Figure 4. Crack pattern of each test specimen

Table 5. Experimental results

Specimen	Observed results				Ultimate load, $P_{u,exp}$ (kN)	Measured results		
	First shear crack, $P_{ic,s}$ (kN)	First flexural crack, $P_{ic,f}$ (kN)	Crack reached opening, $P_{ic,o}$ (kN)	Failure mode		Displacement (mm)		
					At point load 1, $\delta_{1,u}$	At mid-span, $\delta_{2,u}$	At point load 2, $\delta_{3,u}$	
C1/S	96	47	-	F	163.1	8.53	10.20	9.17
C2/F	34	34	-	F	156.8	9.62	10.42	10.09
S1/100	44	39	46	S	108.0	5.20	5.76	5.56
S2/75	69	38	70	S	126.7	6.35	6.99	6.79
S3/50	85	30	126	S	135.8	8.71	9.34	9.17
F1/100	40	33	40	F/S	102.3	8.36	8.61	8.15
F2/75	50	39	125	F/S	127.2	8.12	8.30	8.01
F3/50	69	30	44	F/S	134.3	9.52	10.07	9.42
R1/DR	52	40	89	F	141.1	17.86	17.65	14.39
R2/GI	53	43	71	S	101.6	7.39	7.89	7.90
R3/DS	54	32	81	S	119.0	8.76	9.59	9.17

F – flexural failure, S – shear failure, F/S – flexural and shear failure

Properties of Beam

The properties of the beam were acquired from the load-displacement ($P-\delta$) curves (Figure 5) based on the method proposed by [26] and [27] (Figure 6 and Table 6), as summarized in Table 7.

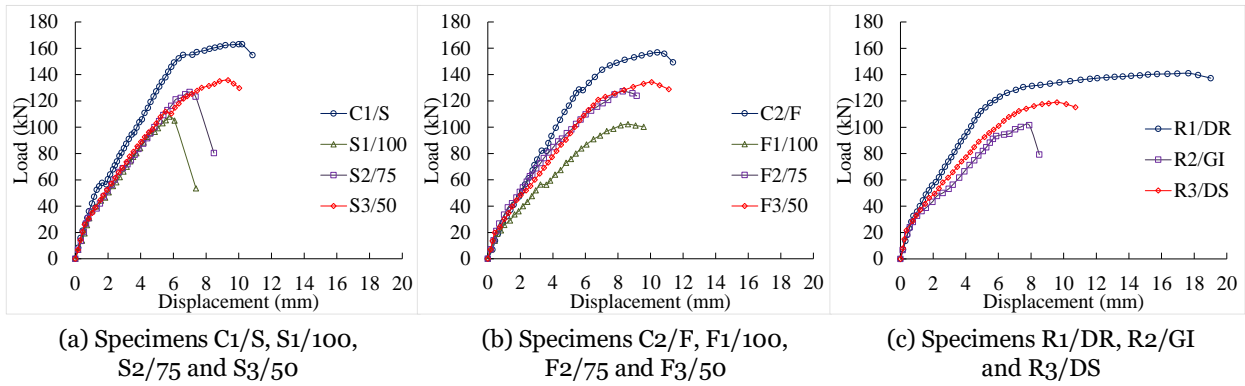


Figure 5. Load-displacement response

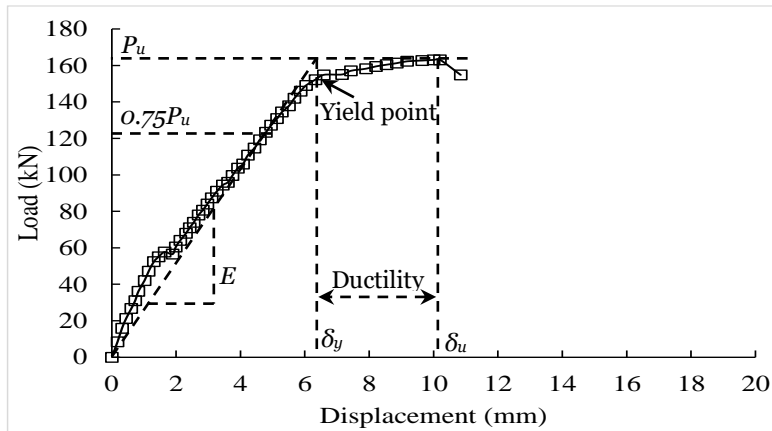


Figure 6. Beam properties of a typical load-displacement response

Table 6. Properties of the beam computed from the load-displacement curve

	Description	Representation in the $P-\delta$ curve
Ultimate load, P_u	Maximum load capacity of the beam.	The highest point on the y-axis.
Ultimate displacement, δ_u	Total displacement of the beam before failure.	The displacement on the x-axis corresponding to P_u .
Secant stiffness, E^*	Resistance to deflection, considering stiffness reduction due to cracking.	Slope of the line from the origin to the point where the horizontal line at $0.75P_u$ intersects the $P-\delta$ curve.
Yield point (P_y, δ_y)*	End of elastic deformation.	Point on the $P-\delta$ curve where the secant stiffness line intersects the horizontal line at P_u .
Ductility, Δ	Ability to deform during the post-yield stage.	Ratio of δ_u to δ_y .

*Determined based on methods proposed by [26] and [27]

Table 7. Properties and performance ratios of beam specimens

Specimen	Secant stiffness, E (kN/mm)	Yield strength, P_y (kN)	Yield Displacement, δ_y (mm)	Performance ratios					
				P_{ic}/P_y	P_{ic}/P_u	$P_{ic,o}/P_y$	$P_{ci,o}/P_u$	P_y/P_u	δ_u/δ_y
C1/S	25.6	152.7	6.37	0.31	0.29	-	-	0.94	1.60
C2/F	23.3	139.8	6.72	0.24	0.22	-	-	0.89	1.55
S1/100	21.6	98.3	4.99	0.40	0.36	0.47	0.43	0.91	1.15
S2/75	20.8	120.2	6.09	0.32	0.30	0.58	0.55	0.95	1.15
S3/50	20.8	120.5	6.52	0.25	0.22	1.05	0.93	0.89	1.43
F1/100	14.9	93.4	6.85	0.35	0.32	0.43	0.39	0.91	1.26
F2/75	19.6	102.3	6.48	0.38	0.31	1.22	0.98	0.80	1.28
F3/50	18.8	122.7	7.15	0.24	0.22	0.36	0.33	0.91	1.41
R1/DR	23.2	123.1	6.08	0.32	0.28	0.72	0.63	0.87	2.90
R2/GI	16.6	94.0	6.13	0.46	0.42	0.76	0.70	0.93	1.29
R3/DS	18.5	106.0	6.45	0.30	0.27	0.76	0.68	0.89	1.49

Table 8. Evaluation of the beam performance with respect to the control specimens

	Specimen	First crack	Stiffness	Yield strength	Ultimate strength	Yielding displacement	Ultimate displacement	Ductility
		$P_{ic,i}/P_{ic,c}$	E_i/E_c	$P_{y,i}/P_{y,c}$	$P_{u,i}/P_{u,c}$	$\delta_{y,i}/\delta_{y,c}$	$\delta_{u,i}/\delta_{u,c}$	Δ_i/Δ_c
Effects of opening near the support under shear load	C1/S	1.00	1.00	1.00	1.00	1.00	1.00	1.00
	S1/100	0.83	0.84	0.64	0.66	0.78	0.56	0.72
	S2/75	0.81	0.81	0.79	0.78	0.96	0.69	0.72
	S3/50	0.64	0.81	0.79	0.83	1.02	0.92	0.89
Effects of opening at mid span under flexural load	C2/F	1.00	1.00	1.00	1.00	1.00	1.00	1.00
	F1/100	0.97	0.64	0.67	0.65	1.02	0.83	0.81
	F2/75	1.15	0.84	0.73	0.81	0.96	0.80	0.83
	F3/50	0.88	0.81	0.88	0.86	1.06	0.97	0.91
Effects of reinforcement for opening under shear load	S1/100	1.00	1.00	1.00	1.00	1.00	1.00	1.00
	R1/DR	1.03	1.07	1.25	1.31	1.22	3.06	2.52
	R2/GI	1.10	0.77	0.96	0.94	1.23	1.37	1.12
	R3/DS	0.82	0.86	1.08	1.10	1.29	1.66	1.3

Performance of beam

The beam properties were then re-computed into several ratios to represent the performance of the beams (Table 7). These ratios reflect:

- the occurrence of the first cracks relative to the yielding or ultimate strengths (i.e., P_{ic}/P_y , P_{ic}/P_u , $P_{ic,o}/P_y$, and $P_{ic,o}/P_u$),
- the yield strength relative to the ultimate strength (i.e., P_y/P_u), and
- the ductility of the specimens (i.e., δ_u/δ_y).

The beams with openings were then compared with the solid beams by weighting their properties (stiffness, yield strength, ultimate strength, yield displacement, ultimate displacement, and ductility) against the control specimens (C1/S, C2/F, and S1/100), as presented in Table 8. This comparison demonstrates the parametric response of the openings.

BEHAVIOUR OF BEAMS WITH OPENING

The behaviour of the beams is discussed in terms of (a) the load-displacement (P - δ) response, (b) the failure mode, (c) the effects of the opening, and (d) the effects of the reinforcements for the opening.

Load-Displacement Response

Two types of P - δ responses were observed in Figure 5: ductile and brittle responses. Generally, beams without openings and those with adequately reinforced openings exhibited ductile responses (Table 9). Beams with improperly reinforced or unreinforced openings displayed brittle responses.

The main difference between these responses was in the post-yielding stage. Beams with brittle responses failed almost immediately after the yield point, while those with ductile responses endured significant deflection before failure.

Table 9. Comparison of load-displacement responses of test specimens

Types	Ductile response	Brittle response
Specimens	C1/S, C2/F, F3/50, R1/DR	S1/100, S2/75, S3/50, F1/100, F2/75, R2/GI, R3/DS
Characteristics of the specimens	<ul style="list-style-type: none"> • Beams without opening, or • Beams with small unreinforced openings at mid-span, or • Beams with large, appropriately reinforced openings near support 	<ul style="list-style-type: none"> • Beams with opening near support, or • Beams with large unreinforced openings at mid-span, or • Beams with large, poorly reinforced openings near support
Uncracked stage	The beams showed high stiffness and behaved elastically. Deflection increased gradually and proportionally with larger loads. Both the concrete and the reinforcement bars contributed to the beam's load resistance.	
Cracked stage	The concrete's deformability limit was exceeded, leading to the first flexural crack at the mid-span. As a result, the concrete lost some bending strength and stiffness decreased slightly. The beam's strength mainly relied on the still-elastic reinforcement bars, causing deflection to increase proportionally with the load. As the load increased, the number, length, and width of cracks grew. Cracks expanded from the mid-span toward the beam ends until a diagonal shear crack formed.	
Yield point	The stiffness dropped significantly, causing large displacements with small load increments. This could be attributed to (a) excessive cracking of the concrete, disrupting the bond between the reinforcement bars and the concrete, and (b) localized yielding of the reinforcement bars, which accelerated the beam's deflection.	
Post-yield stage	Large displacements developed at a roughly proportional rate for some time before reaching the ultimate state.	The stiffness deteriorated quickly, and the specimen reached the ultimate state almost immediately after the yield point. The displacement at the ultimate state was similar to that at the yielding state.
Ultimate state	Critical damage affected the beam's integrity, leading to a loss of strength.	

Failure Mode

The failure mode indicates the critical causes of failure governing the beam's strength, identified from the crack lines and crack width (Figure 4). Three types of failure modes were observed: flexural, shear, and flexural-shear failures (Table 10). The presence of openings made the beams more vulnerable by:

- Reducing the effective cross-sectional area, led to faster stress accumulation near the opening, resulting in early cracking.
- Shortening the cracking distance from the beam soffit to the compressive zone. Once a crack reached the opening, it quickly propagated to the other side, leading to beam failure.

Table 10. Types of failure mode

Failure mode	Descriptions	Common occurrence	Strength governing factor
Flexural failure	Numerous vertical cracks, angled at 60 degrees or more from the beam soffit, appeared in the middle third of the beam span. These cracks propagated upward from the soffit to the compressive zone. The failure occurred due to excessive elongation of the tension steel bars, surpassing the deformability limit of the concrete, and damage to the bond between the concrete and the tension steel bars. Flexural stress in the beam was more dominant than shear stress.	Solid RC beam (C1/S and C2/F) Beams which are adequately reinforced at the opening (R1/DR)	Bending moment
Shear failure	An inclined crack, angled between 30 and 60 degrees from the beam soffit, propagated from the soffit near the support to the top face of the beam near the point load. The failure occurred because the tensile stress in the compression zone exceeded the concrete's tensile capacity and the bond between the tension steel bars and the concrete at the support was destroyed. Shear stress was more predominant than flexural stress.	Beams with opening near the support without adequate reinforcement (S1/100, S2/75, S3/50, R2/GI, R3/DS)	Shear load
Flexural and shear failure	Both flexural and shear cracks were exhibited with similar severity. The failure occurred due to either flexural or shear failure, depending on which had the lower capacity.	Beams with opening at the mid-span without adequate reinforcement (F1/100, F2/75 and F3/50)	Bending moment or shear load

Effects of opening

Openings generally reduced the stiffness, yield strength, ultimate strength, deflection, and ductility of the beams (Table 11). These effects were detrimental to beam and amplified with increasing opening size (Table 12). The main cause was stress concentration due to the reduced effective cross-sectional area.

Table 11. Effects of opening in beam in comparison with the control specimens

Responses* ¹	Location of the opening	
	Near the support (under shear load)	At mid-span (under flexural load)
First crack	Occurred slightly earlier than the control specimen* ²	No specific trend observed
Secant stiffness	Reduced by about 20% stiffness	Reduced. The stiffness was more significantly affected by a large opening (100 mm dia.)* ²
Yield strength	Reduced* ²	
Ultimate strength	Reduced* ²	
Deflection at the yielding stage	Slightly affected with a small opening (≤ 75 mm dia.). More significantly affected by large opening (about 22% reduction for 100 mm dia.)* ² .	Negligible effects
Deflection at the ultimate state	Reduced allowable deflection up to 44%* ²	Reduced allowable deflection, up to 20%
Ductility*	Reduced. The ductility reduced more significantly up to 28%* ²	Reduced up to 19% ductility

¹The responses were observed from the results given in Table 5 and Table 8.

²Relatively unfavourable condition in terms of beam performance

Table 12. Effects of increasing opening size

Response* ¹	Location of the opening	
	Near the support (under shear load)	At mid-span (under flexural load)
First crack	The occurrence of the first crack delayed	No specific trend observed
The first crack reached the opening	The crack reached the opening at a lower load* ²	No specific trend observed
Secant stiffness	Insignificant effect	Reduced* ²
Yield strength	Reduced* ²	
Ultimate strength	Reduced* ²	
Deflection at the yielding stage	Reduced* ²	Insignificant effect
Deflection at the ultimate state	Reduced more significantly* ²	Reduced
Ductility	Reduced more significantly* ²	Reduced

¹The responses were observed from the results given in Table 5 and Table 8.

²Relatively unfavourable condition in terms of beam performance

The main difference between these responses was in the post-yielding stage. Beams with brittle responses failed almost immediately after the yield point, while those with ductile responses endured significant deflection before failure.

Beams with openings were more critically affected under shear loads than flexural loads, as evident by:

- The detrimental effects on most aspects listed in Table 11 were more severe under shear loads compared to flexural loads.
- The negative impact of increasing opening size was more pronounced under shear loads (Table 12).

Effect of reinforcements for opening

Table 13 compares the effectiveness of three reinforcement methods for openings. The diagonal bar reinforcement was found to be the most effective, outperforming the other methods in all aspects.

In terms of failure mode:

- The diagonal bar reinforcement controlled the shear crack at the opening better than the other methods (Figure 4(i)), making the beam with the opening stronger.
- The diagonal square reinforcement disrupted the first diagonal shear crack but could not control subsequent cracks, which propagated at higher loads and bypassed the reinforcement (Figure 4(k)).
- The GI pipe reinforcement increased the compressive strength at the opening but did not control diagonal shear cracks. At the ultimate state, cracks propagated through the opening to the top face of the beam (Figure 4(j)).

Table 13. Comparison of the performance of different reinforcing methods

Responses* ¹	Reinforcing method for opening		
	Diagonal bar reinforcement	GI pipe reinforcement	Diagonal square reinforcement
Specimen	R1/DR	R2/GI	R3/DS
First crack reached opening	Significantly increased (+93%)* ²	Increased (+54%)	Significantly increased (+76%)
Secant stiffness	Slightly increased (+3%)* ²	Significantly decreased (-23%)	Decreased (-14%)
Yield strength	Significantly increased (+25%)* ²	Insignificant effect (-4%)	Slightly increased (+8%)
Ultimate strength	Significantly increased (+31%)* ²	Insignificant effect (-4%)	Slightly increased (+10%)
Deflection at the yielding stage	Increased 22% to 29%* ²		
Deflection at the ultimate state	Significantly increased (3.06 times)* ²	Slightly increased (37%)	Moderately increased (66%)
Ductility	Significantly increased (2.52 times)* ²	Slightly increased (12%)	Moderately increased (30%)

¹The responses were observed from the results given in Table 8

²The most favourable conditions of all reinforcing methods

Appropriate reinforcements for openings can increase load resistance (e.g., crack resistance, stiffness, yield strength, ultimate strength), deflection, and ductility of the beam. Inappropriate reinforcements, however, should theoretically have negligible effects (neither helpful nor harmful).

The evaluation of different reinforcement methods for openings leads to the following principles:

- Reinforcements should control the propagation of cracks rather than just strengthening the opening itself.
- Reinforcement bars should be aligned perpendicularly to potential cracks.
- Reinforcement bars should cover a wider region, not just surround the opening.

Based on these principles, reinforcement bars for openings could be arranged as illustrated in Figure 7, taking into account the potential directions of cracks. This arrangement ensures that the reinforcement effectively addresses the structural weaknesses introduced by the openings, providing enhanced stability and performance under load.

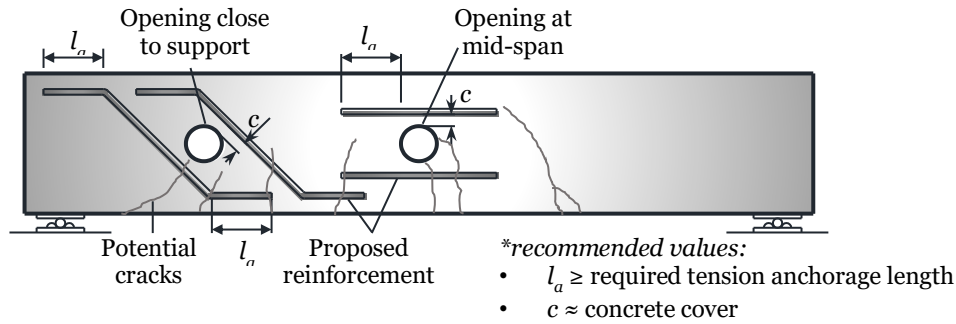


Figure 7. Proposed reinforcements for opening in RC beam

ANALYTICAL MODEL

An analytical model was derived to predict the shear strength, flexural strength, load capacity, and failure mode of beams with openings.

Shear strength of a beam with opening

The overall shear strength ($V_{u,pre}$), referring to [12] and [28], was determined based on the contributions from concrete (V_c), shear reinforcement (V_{sl}), and diagonal reinforcement (V_{sd}), as given by:

$$V_{u,pre} = V_c + V_{sl} + V_{sd} \quad (1)$$

a. Contribution from Concrete

The shear strength provided by the concrete (V_c) is calculated as:

$$V_c = 0.17\sqrt{f_{c,u,c}}b_b(d_b - d_o) \quad (2)$$

where $f_{c,u,c}$ is the compressive stress of the concrete cylinder (N/mm²)

b_b is the width of the beam (mm)

d_b is the depth of the beam (mm)

d_o is the diameter of the transverse opening (mm)

Since cylinder strength, $f_{c,u,c}$, was not tested, it was determined by interpolating the cube strength, $f_{c,u}$ (Table 3), based on the standard concrete grades of Eurocode 2 (C20/25, C25/30, and C30/37).

b. Contribution from Shear Reinforcement

The contribution from the shear reinforcement (V_{sl}) is given by:

$$V_{sl} = \frac{A_{sl}f_{sl}}{s}(d_v - d_o) \quad (3)$$

where A_{sl} is the cross-sectional area of the shear links (mm²)

f_{sl} is the tensile stress in the shear links (N/mm²)

s is the spacing of the shear links (mm)

d_v is the center-to-center distance between the top and bottom reinforcement (mm)

The effective depth (d_v) is determined by: (Figure 8)

$$d_v = h_b - 2c - 2\phi_{sl} - \frac{\phi_{bb}}{2} - \frac{\phi_{tb}}{2} \quad (4)$$

where h_b is the height of the beam (mm)

c is the concrete cover (mm)

ϕ_{sl} is the diameter of the shear link (mm)

ϕ_{bb} is the diameter of the bottom steel bar (mm)

ϕ_{tb} is the diameter of the top steel bar (mm)

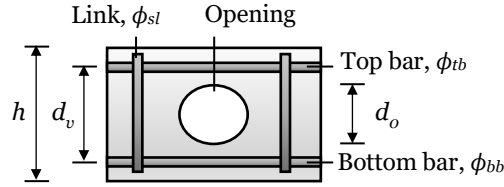


Figure 8. Effective depth, d_v

c. Contribution from Diagonal Reinforcement

The contribution from the diagonal reinforcement (V_{sd}) is given by:

$$V_{sd} = k_{sd} A_{sd} f_{sd} \sin \alpha \quad (5)$$

where: k_{sd} is the coefficient for reinforcing methods

A_{sd} is the cross-sectional area of the diagonal reinforcement bars (mm²)

f_{sd} is the tensile stress in the diagonal reinforcement bars (N/mm²)

α is the angle of the diagonal bar reinforcement (rad)

The coefficient k_{sd} represents the effectiveness of the different reinforcing methods:

- The diagonal bar reinforcing method is the most effective ($k_{sd} = 1.0$).
- The GI reinforcing method does not strengthen the opening ($k_{sd} = 0$).
- The diagonal square reinforcing method offers some shear strength but is less effective than the diagonal bar method. Thus, k_{sd} is assumed to be 0.1 to align the predicted load capacity with experimental results.

d. Coefficient k_{sl} and k_{st}

The tensile stresses of the shear link (f_{sl}) and the diagonal reinforcement bar (f_{sd}) are computed by:

$$f_{sl} = k_{sl} f_{y,sl} \quad (6)$$

$$f_{sd} = k_{st} f_{y,sd} \quad (7)$$

Coefficients k_{sl} and k_{st} are factors correlating the yielding strength and the ultimate strength (Eqs. 6 and 7). They were calculated by dividing the average tensile strength (Table 4) by their nominal tensile strengths of 250 N/mm² for $f_{y,sl}$ and 460 N/mm² for $f_{y,sd}$:

- $k_{sl} = 1.14$
- $k_{sd} = 1.18$

Flexural strength of beam with opening

The flexural strength of the beam was predicted based on the stress block diagram shown in Figure 9. The stress block model assumed the following:

- The beam section was singly reinforced.
- The section remained plane after bending, resulting in a linearly distributed strain across the section.

- The section properties were based on the gross concrete section.
- Bending occurred about the neutral axis of the beam section, with its location remaining the same throughout the beam and not being affected by the opening.
- Concrete carried no tensile stress, with all tensile stress taken by the reinforcements.
- The transverse opening was treated as a rectangular void with a height equivalent to its diameter (d_o), assuming a consistent cross-section throughout the beam.
- The PVC and GI pipes used to create the opening did not contribute any strength to the beam.
- For predicting ultimate strength, the materials' ultimate strengths were used with the safety factors set to 1.0.

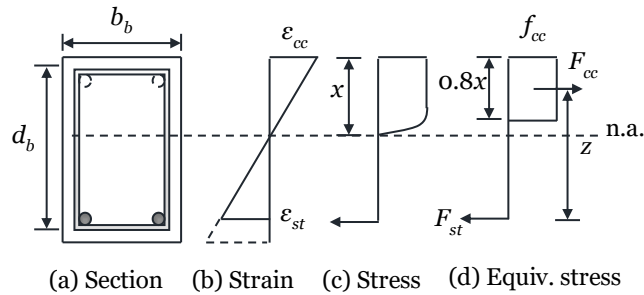


Figure 9. Stress block diagram for a typical beam

From the stress block diagram, the equilibrium equation in the horizontal direction ($\sum F_x = 0$) is:

$$F_{cc} - F_{st} = 0 \quad (8)$$

where $F_{cc} = 0.8x f_{cc} b_b$ (9)

$$F_{st} = f_{st} A_{st} \quad (10)$$

The neutral axis was derived from Eq. (8) as follows:

$$x = \frac{1.25 f_{st} A_{st}}{f_{cc} b_b} \quad (11)$$

where $f_{cc} = k_{cc} \frac{f_{c,u,c}}{\gamma_c}$ (12)

$$f_{st} = k_{st} f_{y,b} \quad (13)$$

Constants; $k_{cc} = 0.85$, $\gamma_c = 1.0$, $k_{st} = 1.18$

The coefficient k_{cc} correlates compressive and flexural strength of concrete. For concrete strengths, $f_{c,u,c}$ between 17.2 N/mm² and 27.6 N/mm², k_{cc} is taken as 0.85 (ACI-318-14).

The moment resistance of the beams is given by:

$$M_{u,pre} = F_{st} Z \quad (14)$$

where $F_{st} = f_{st} A_{st}$ (15)

$$z = d_b - 0.4x \quad (16)$$

Load capacity of beam with opening

Figure 10 shows the free-body diagram of the test setup, assuming two point loads of magnitude $P_u/2$ acting on the beam and the self-weight of the beam as a uniformly distributed load, w . The maximum shear occurs at the support, as expressed in Eq. 17, and the maximum moment develops at the mid-span, as given in Eq. 18.

$$V = \frac{P_u}{2} + \frac{wl}{2} \quad (17)$$

$$M = \frac{1}{2} \left(P a + \frac{wl^2}{4} \right) \quad (18)$$

where w is the self-weight of the beam, $w = b_b \cdot h_b \cdot \gamma_{cb}$ and γ_{cb} is the unit weight of concrete, 25 kN/m³

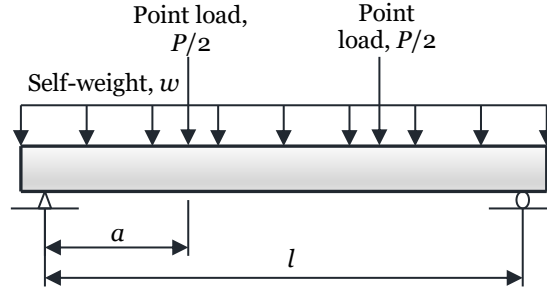


Figure 10. The free-body diagram of the test setup

The beam's load capacity was determined by the first limit reached between shear strength, $P_{u,v}$, and flexural strength, $P_{u,M}$.

$$P_{u,pre} = \min\{P_{u,v}, P_{u,M}\} \quad (19)$$

$P_{u,v}$ and $P_{u,M}$ represent the equivalent loads acting on the beam based on the experimental setup in terms of the shear and flexural strengths, $V_{u,pre}$ and $M_{u,pre}$, respectively. Eqs. 20 and 21 were derived from Eqs. 17 and 18, respectively.

$$P_{u,v} = 2V_{u,pre} - wl \quad (20)$$

$$P_{u,M} = \frac{1}{a} \left(2M_{u,pre} - \frac{wl^2}{4} \right) \quad (21)$$

Failure mode of beam with opening

The beam's failure mode was predicted by comparing the predicted shear strength ($P_{u,v}$), the predicted moment strength ($P_{u,M}$), and the average of these strengths ($P_{u,avg}$) (Table 14).

- If the predicted shear strength was significantly less than the predicted moment strength by more than 10% of their average value, shear failure was assumed.
- Conversely, if the predicted moment strength was significantly less than the predicted shear strength by more than 10% of their average value, flexural failure was assumed.
- If the difference between the predicted strength (either shear or moment) and the average was within 10%, the specimen was considered to experience shear and flexural failure at approximately the same time.

Table 14. Equation conditions for predicting the failure mode of the specimens

Failure mode	Equation conditions	Description
Shear failure	$P_{u,v} < P_{u,M}$ and $ P_{u,v} - P_{u,avg} > 0.1P_{u,avg}$	The shear strength was significantly lower than the flexural strength.
Shear and flexural failure	$ P_{u,v} - P_{u,avg} \leq 0.1P_{u,avg}$ or $ P_{u,M} - P_{u,avg} \leq 0.1P_{u,avg}$	The shear strength and flexural strength were about the same.
Flexural failure	$P_{u,v} > P_{u,M}$ and $ P_{u,M} - P_{u,avg} > 0.1P_{u,avg}$	The flexural strength was significantly lower than the shear strength.

Verification of analytical model

The predicted shear strength, moment strength, loading capacity and failure mode are computed in Table 15 to Table 18.

Table 15. Predicted shear strength of the beam

Specimen	Cylinder strength, $f_{c,u,c}$ (N/mm ²)	Concrete shear strength, V_c (kN)	Shear link, A_{sl}/s	Shear reinf., V_{sl} (kN)	Area of opening reinf., A_{sd} (mm ²)	Coeff. k_{sd}	Opening reinf., V_{sd} (kN)	Predicted shear strength, $V_{u,pre}$ (kN)
Ref.	Eq. 2	Eq. 2	Eq. 3	Eq. 3	Eq. 5	Eq. 5	Eq. 1	
C1/S	20.1	29.8	0.402	25.5	0	0	0	55.3
C2/F	21.0	30.5	0.670	42.6	0	0	0	73.1
S1/100	19.7	18.2	0.402	14.1	0	0	0	32.3
S2/75	19.9	21.2	0.402	17.0	0	0	0	38.2
S3/50	20.4	24.3	0.402	19.8	0	0	0	44.1
F1/100	20.8	18.7	0.670	23.5	0	0	0	42.2
F2/75	20.0	21.2	0.670	28.3	0	0	0	49.5
F3/50	22.0	25.2	0.670	33.0	0	0	0	58.2
R1/DR	21.8	19.2	0.402	14.1	226	1	86.8	120.1
R2/GI	21.3	18.9	0.402	14.1	0	0	0	33.0
R3/DS	20.9	18.8	0.402	14.1	226	0.1	8.68	41.6

d_o refer to Table 1, $f_{c,u}$ refer to Table 3, $b_b = 150$ mm, $d_b = 261$ mm, $k_{sl} = 1.14$, $f_{y,sl} = 250$ N/mm², $f_{sl} = 285$ N/mm² (Eq. 6), $d_v = 223$ mm (Eq. 4), $k_{st} = 1.18$, $f_{y,sd} = 460$ N/mm², $f_{sd} = 543$ N/mm², $\alpha = 45^\circ$

Table 16. Predicted flexural strength of the beam

Specimen	Compressive stress, f_{cc} (N/mm ²)	Neutral axis, x (mm)	Lever arm, z (mm)	Predicted moment, $M_{u,pre}$ (kNm)
Reference	Eq. 12	Eq. 11	Eq. 16	Eq. 14
C1/S	17.1	59.8	237	29.1
C2/F	17.9	57.1	238	29.2
S1/100	16.7	61.2	237	29.1
S2/75	16.9	60.5	237	29.1
S3/50	17.3	59.1	237	29.1
F1/100	17.7	57.8	238	29.2
F2/75	17.0	60.2	237	29.1
F3/50	18.7	54.7	239	29.3
R1/DR	18.5	55.3	239	29.3
R2/GI	18.1	56.5	238	29.2
R3/DS	17.8	57.5	238	29.2

$f_{st} = 543$ N/mm² (Eq. 13), $A_{st} = 226$ mm², $k_{cc} = 0.85$, $\gamma_c = 1.0$, $f_{c,u,c}$ refer to Table 15, $b_b = 150$ mm, $d_b = 261$ mm, $F_{st} = 122.7$ kN (Eq. 15)

Table 17. Predicted loading capacity of beam

Specimen	Shear strength, $P_{u,v}$ (kN)	Moment, $P_{u,M}$ (kN)	Predicted load capacity, $P_{u,pre}$ (kN)	Experimental load capacity, $P_{u,exp}$ (kN)	$R_p = P_{u,pre}/P_{u,exp}$	Remark
Ref.	Eq. 20	Eq. 21	Eq. 19	Table 5	Eq. 22	
C1/S	108.9	115.1	108.9	163.1	0.67	NA
C2/F	144.5	96.3	96.3	156.8	0.61	NA
S1/100	62.9	115.1	62.9	108	0.58	NA
S2/75	74.7	115.1	74.7	126.7	0.59	NA
S3/50	86.5	115.1	86.5	135.8	0.64	NA
F1/100	82.7	96.3	82.7	102.3	0.81	NA
F2/75	97.3	95.9	95.9	127.2	0.75	NA
F3/50	114.7	96.6	96.6	134.3	0.72	NA
R1/DR	238.5	115.9	115.9	141.1	0.82	NA
R2/GI	64.3	115.5	64.3	101.6	0.63	NA
R3/DS	81.5	115.5	81.5	119.0	0.68	NA

Mean = 0.68 Reliability = 0/11

$V_{u,pre}$ refer to Table 15, $M_{u,pre}$ refer to Table 16, $w = 1.125$ kN/m, $l = 1.5$ m, a refer to Table 1

A – Applicable ($0.9 \leq R_p \leq 1.1$), NA – Not Applicable ($R_p < 0.9, > 1.1$)

Table 18. Predicted failure mode of beam

Specimen	Predicted failure mode	Experimental failure mode	Remark
Ref.	Table 14	Table 5	
C1/S	F/S	F	NA
C2/F	F	F	A
S1/100	S	S	A
S2/75	S	S	A
S3/50	S	S	A
F1/100	F/S	F/S	A
F2/75	F/S	F/S	A
F3/50	F/S	F/S	A
R1/DR	F	F	A
R2/GI	S	S	A
R3/DS	S	S	A

Reliability = 10/11

F – flexural failure, S – shear failure, F/S – flexural and shear failure

A – Applicable (predicted failure mode = experimental failure mode), NA – Not Applicable (predicted failure mode ≠ experimental failure mode)

For verification of the analytical model, the predicted loading capacity and failure mode were compared with the experimental results. The model was considered reliable when a majority of the specimens ($\geq 80\%$) had (a) the predicted ultimate load within $\pm 10\%$ variation from the experimental results ($0.9 \leq R_p \leq 1.1$), and (b) the predicted failure mode in line with the observation in the experiment [29-30].

$$R_p = \frac{P_{u,pre}}{P_{u,exp}} \quad (22)$$

Based on the predicted outcomes:

- The analytical model inaccurately predicted the load capacity of beams with a transverse opening. None of the specimens had an R_p ratio between 0.9 and 1.1.
- The prediction was generally conservative, with an R_p ratio of less than 1.0 and a mean R_p ratio of 0.68.
- The prediction was more conservative for specimens more dominant in shear. The R_p ratios of S1/100, S2/75, and S3/50 were all lower than those of specimens F1/100, F2/75, and F3/50 with the same opening size.
- The model correctly predicted 10 out of 11 failure modes of the specimens (90.9%). Its accuracy was higher than that of the model used by [22], which correctly predicted the failure mode for 54.5% of specimens.

An opening decreases a beam's cross-section and thus reduces its load capacity, as reflected by d_o being deducted from d_v in Eq. 2. For safety, brittle failure should be avoided by designing the shear strength to be slightly higher than the moment capacity. According to the equation model, shear strength can be increased by:

- Increasing the area of the shear links and diagonal reinforcement, A_{sl} and A_{sd}
- Increasing the concrete and steel grades, $f_{c,u,c}$, f_{sl} , and f_{sd}
- Reducing the spacing between the shear links, s

In this study, 150 mm concrete cubes were tested for compressive strength. However, the equation model used 150 mm x 300 mm cylinder strength, estimated through interpolation from cube strength. Cylinder strength was chosen for its theoretical validity and alignment with Eurocode 2, while cube testing reflects local industry practices. Although interpolation ensures compatibility, it may reduce accuracy. Future studies should prioritize direct cylinder testing for improved reliability and model validation.

The equation for predicting the beam's shear strength (Eq. 1) was a simplified model that ignored the effects of the dowel action of the longitudinal bars and the moment-to-shear ratio of the section. These factors are considered in the detailed methods given by [12] and [28]. A slightly higher shear strength is expected from the detailed methods, making the predicted load capacity of the beam more accurate and less conservative.

The neutral axis, x , was calculated based on a solid singly reinforced beam and was assumed to be constant throughout the beam, unaffected by the openings. Since all openings were located below the

neutral axis and did not disturb the $0.8x$ equivalent stress block, their influence on the moment capacity was ignored. Thus, the model only considers openings affecting the shear strength, not the moment capacity.

In a simply supported beam, the maximum shear occurs at the supports, and the maximum moment occurs at the mid-span. The equation model predicts load capacity based on the smaller value of the beam's shear strength and moment capacity, regardless of the opening's location. The model may be applicable for cantilevers and continuous beams where maximum shear and moment occur at the same place, but this was not verified in this study. Future studies could refine the model by considering the location of the opening and testing its applicability in various types of beams.

The model accounts for the beam's load capacity affected by openings but lacks refinement regarding its range of applicability. It predicts the load capacity of a beam with a single opening similar to one with multiple openings, regardless of the shape. Factors like the number, shape, size, and aspect ratio of openings, as well as the spacing between openings, may affect the beam's load capacity. Future studies should explore these aspects.

From Table 16, the neutral axis was found to range from 54.7 mm to 61.2 mm from the top of the beam, about 0.2 times the beam height. To avoid disturbing the neutral axis, the opening size should not exceed 0.6 times the beam height (Figure 11). In this study, the largest opening size used was 100 mm, one-third of the beam height. Therefore, the analytical model is deemed applicable for predicting the failure mode and conservatively predicts the load capacity of simply supported beams that are singly reinforced with an opening size not exceeding one-third of their height. Further study may be required to verify this.

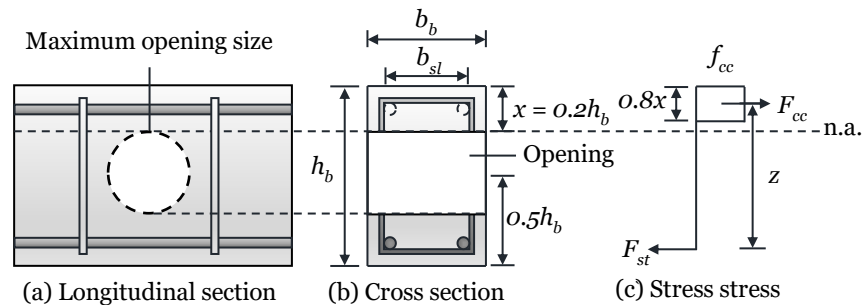


Figure 11. Maximum opening size

The coefficients k_{sd} for different reinforcing methods, especially $k_{sd} = 0.1$ for the diagonal square reinforcing method, were assumed values not based on first principles or any statistical approach. The sampling size was relatively small, with only one specimen for each reinforcement method. A more representative k_{sd} may be determined using a more rigorous approach with a larger sampling size.

CONCLUSION

In this study, reinforced concrete beams with transverse openings were investigated both experimentally and analytically to understand their structural behaviour and predict their performance.

From the experimental study, the following conclusions were drawn:

- Openings reduced the beam's stiffness, yield strength, and ultimate strength.
- Openings encouraged shear failure, negatively affecting the beam's ductility response.
- These detrimental effects were more pronounced when: (i) the opening was placed near the support, (ii) a large opening size was used, and (iii) the opening was inadequately reinforced.
- The diagonal bar reinforcing method was the most effective in strengthening beams with openings.

From the analytical study, the following conclusions were drawn:

- The analytical model inaccurately but conservatively predicted the beams' load capacity, with a mean R_p ratio of 0.68.

- b. The model correctly predicted 10 out of 11 failure modes of the specimens (90.9%).

While this study highlights the significant impact of transverse openings on beams' performance, its scope is limited to conditions involving a single circular opening not exceeding one-third of the beam's height on a simply supported beam. Future studies should experimentally and analytically explore the influence of multiple openings of various shapes and sizes greater than one-third of the beam height to further contribute to the body of knowledge.

ACKNOWLEDGEMENT

This work was supported by the Research Grants of the University of Technology Sarawak, UCTS/RESEARCH/2/2018/02.

REFERENCES

- [1] L. Herrera, S. Anacleto-Lupianez, and A. Lemnitzer, "Experimental performance of RC moment frame beams with rectangular openings," *Engineering Structures*, vol. 152, pp. 149-167, 2017, doi: 10.1016/j.engstruct.2017.08.043.
- [2] M.A. Mansur, "Design of reinforced concrete beams with web openings," *6th Asia-Pacific Structural Engineering and Construction Conference (APSEC 2006)*, Kuala Lumpur, Malaysia, pp. 104-120, 2006.
- [3] B. Aykac, I. Kalkan, S. Aykac, and Y.E. Egriboz, "Flexural behavior of RC beams with regular square or circular web openings," *Engineering Structures*, vol. 56, pp. 2165-2174, 2013, doi: 10.1016/j.engstruct.2013.08.043.
- [4] N.K. Oukaili, and A.H. Al-Shammari, "CFRP strengthening of RC beams with multiple openings subjected to static and impact loads," *Advances in Structural Engineering*, vol. 17, no. 12, pp. 1747-1760, 2014, doi: 10.1260/1369-4332.17.12.1747.
- [5] S. Mamatha, N. Changler, P. Singore, S.S. Jevoora, and L. Geetha, "The study of behavior of RC beam with transverse opening under static load," *International Journal of Engineering Science and Computing*, vol. 7, no. 6, pp. 13480-13484, 2017.
- [6] A. El-kareim Shoeib, and A. El-sayed Sedawy, "Shear strength reduction due to introduced opening in loaded RC beams," *Journal of Building Engineering*, vol. 13, pp. 28-40, 2017, doi: 10.1016/j.jobe.2017.04.004
- [7] B.H. Osman, E. Wu, B. Ji, and S.S. Abdulhameed, "Shear behavior of reinforced concrete (RC) beams with circular web openings without additional shear reinforcement," *KSCCE Journal of Civil Engineering*, vol. 21, no. 1, pp. 296-306, 2016, doi: 10.1007/s12205-016-0387-7.
- [8] T. El Maaddawy, and S. Sherif, "FRP composites for shear strengthening of reinforced concrete deep beams with openings," *Composite Structures*, vol. 89, no. 1, pp. 60-69, 2009, doi: 10.1016/j.compstruct.2008.06.022.
- [9] H. Abdalla, A.M. Torkey, H.A. Haggag, and A.F. Abu-Amira, "Design against cracking at openings in reinforced concrete beams strengthened with composite sheets," *Composite Structures*, vol. 60, pp. 197-204, 2003, doi: 10.1016/S0263-8223(02)00305-7.
- [10] J.H. Ling, H.S. Tang, W.K. Leong, H.T. Sia, "Effects of transverse circular opening in reinforced concrete beam subjected to incremental static load," *Borneo Journal of Sciences and Technology*, vol. 1, no. 2, pp. 39-44, 2019, doi: 10.35370/BJOST.2019.1.2-06.
- [11] A. Ahmed, M.M. Fayyadh, S. Naganathan, and K. Nasharuddin, "Reinforced concrete beams with web openings: A state of the art review," *Materials & Design*, vol. 40, pp. 90-102, 2012, doi: 10.1016/j.matdes.2012.03.001.
- [12] M.A. Mansur, and K.H. Tan, "Concrete beams with openings: Analysis and design," *Taylor & Francis*, 1999.
- [13] N.F. Somes, and W.G. Corley, "Circular openings in webs of continuous beams," *Special Publication*, vol. 42, 1974, doi: 10.14359/17293.
- [14] A.R. Mohamed, M.S. Shoukry, and J.M. Saeed, "Prediction of the behavior of reinforced concrete deep beams with web openings using the finite element method," *Alexandria Engineering Journal*, vol. 53, no. 2, pp. 329-339, 2014, doi: 10.1016/j.aej.2014.03.001.
- [15] M.R. Osman, K. Metwally, and M.S. Wafaa, "Proposed recommendations for the design of reinforced concrete beams with openings," *The 2015 World Congress on Advances in Structural Engineering and Mechanics (ASEM15)*, Incheon, Korea, 2015.

- [16] S. Amiri, and R. Masoudnia, "Investigation of the opening effects on the behavior of concrete beams without additional reinforcement in opening region using FEM method," *Australian Journal of Basic and Applied Sciences*, vol. 5, no. 5, pp. 617-627, 2011.
- [17] M.S. Latha, and B.M. Naveen Kumar, "Behavior of reinforced concrete beam with opening," *International Journal of Civil Engineering and Technology*, vol. 8, no. 7, pp. 581-593, 2017.
- [18] S.A. Al-Sheikh, "Flexural behavior of RC beams with opening," *Concrete Research Letters*, vol. 5, no. 2, pp. 812-824, 2014, doi: 10.20528/cjcr1
- [19] M. Venugopal, "Behaviour of GFRP retrofitted rectangular RC beams with small web openings under torsion: experimental study," Department of Civil Engineering, National Institute of Technology, Rourkela, India, 2014.
- [20] N.H. Saksena, P.G. Patel, "Experimental study of reinforced concrete beam with web openings," *International Journal of Advanced Engineering Research and Studies*, vol. 2, no. 3, pp. 66-68, 2013.
- [21] N. Torunbalci, "Behaviour and design of large rectangular openings in reinforced concrete beams," *Architectural Science Review*, vol. 45, no. 2, pp. 91-96, 2002, doi: 10.1080/00038628.2002.9697497.
- [22] J.H. Ling, H.S. Tang, W.K. Leong, and H.T. Sia, "Behaviour of reinforced concrete beams with circular transverse openings under static loads," *Journal of Science and Applied Engineering*, 2020, doi: 10.31328/jsae.v3i1.1288.
- [23] S.C. Chin, N. Shafiq, and M.F. Nuruddin, "FRP as strengthening material for reinforced concrete beams with openings – A review," *KSCE Journal of Civil Engineering*, vol. 19, no. 1, pp. 213-219, 2015, doi: 10.1007/s12205-011-0162-8.
- [24] B.H. Osman, E. Wu, B. Ji, A.M. S Abdelgader, "A state of the art review on reinforced concrete beams with openings retrofitted with FRP," *International Journal of Advanced Structural Engineering*, vol. 8, no. 3, pp. 253-267, 2016, doi: 10.1007/s40091-016-0128-7.
- [25] S.B. Kudatini, and H. Eramma, "Experimental investigation on internally strengthened RC beam with rectangular web opening," *International Journal of Innovative Research in Science, Engineering and Technology*, vol. 5, no. 8, pp. 15410-15417, 2016, doi: :10.15680/IJIRSET.2016.0508175
- [26] R. Park, "Ductility evaluation from laboratory and analytical testing," *The 9th World Conference on Earthquake Engineering*, Tokyo-Kyoto, Japan, pp. 605-616, 1988.
- [27] A. Noushini, B. Samali, and K. Vessalas, "Performance of concrete beam elements reinforced with polyvinyl alcohol (PVA) micro fibres," *Concrete in Australia*, vol. 40, no. 1, pp. 22-27, 2014.
- [28] ACI-318-14, "Building code requirements for structural concrete and commentary," *American Concrete Institute Farmington Hills MI*, 2014.
- [29] J.H. Ling, J.T.S. Ngu, Y.T. Lim, W.K. Leong, and H.T. Sia, "Equation model for predicting the load capacity of RC hollow beams," *Borneo Journal of Sciences And Technology*, vol. 5, no. 2, pp. 84-97, 2023, doi: 10.35370/bjost.2023.5.2-09
- [30] J.H. Ling, L.L. Chan, W.K. Leong, and H.T. Sia, "The development of finite element model to investigate the structural performance of reinforced concrete hollow beams," *Journal of the Civil Engineering Forum*, vol. 6, no.2, pp. 171-182, 2020, doi: 10.22146/jcef.53301